USGS
science for a changing world

Geochemical and Petrographic Data for Intrusions Peripheral to the Big Timber Stock, Crazy Mountains, Montana

Data Series 895

U.S. Department of the Interior
U.S. Geological Survey

COVER. Prominent Eocene sill along the ridge crest, above rocks of the Fort Union Formation, 4 kilometers northeast of Gobblers Knob, Montana. (Photo by Anna B. Wilson, U.S. Geological Survey, 1992.)

Geochemical and Petrographic Data for Intrusions Peripheral to the Big Timber Stock, Crazy Mountains, Montana

By Edward A. du Bray, Anna B. Wilson, and Bradley S. Van Gosen

Data Series 895

U.S. Department of the Interior
U.S. Geological Survey

U.S. Department of the Interior
SALLY JEWELL, Secretary

U.S. Geological Survey
Suzette M. Kimball, Acting Director

U.S. Geological Survey, Reston, Virginia: 2015

For more information on the USGS—the Federal source for science about the Earth, its natural and living resources, natural hazards, and the environment, visit http://www.usgs.gov or call 1–888–ASK–USGS.

For an overview of USGS information products, including maps, imagery, and publications, visit http://www.usgs.gov/pubprod

To order this and other USGS information products, visit http://store.usgs.gov

Suggested citation:
du Bray, E.A., Wilson, A.B., and Van Gosen, B.S., 2015, Geochemical and petrographic data for intrusions peripheral to the Big Timber stock, Crazy Mountains, Montana: U.S. Geological Survey Data Series 895, 19 p., *http://dx.doi.org/10.3133/ds895.*

ISSN 2327-638X (online)

Contents

Figures

Tables

Abbreviations

Al_2O_3	aluminum oxide
Am	americium
Ba	barium
CaO	calcium oxide
Cd	cadmium
Ce	cerium
FeO	ferrous iron
K	potassium
K_2O	potassium oxide
La	lanthanum
MgO	magnesium oxide
MnO	manganese oxide
Na_2O	sodium oxide
Nb	niobium
Nd	neodymium
P_2O_5	phosphorus pentoxide
Rb	rubidium
SiO_2	silicon dioxide
Sr	strontium
TiO_2	titanium dioxide
Y	yttrium
Zr	zirconium
ppm	parts per million

Geochemical and Petrographic Data for Intrusions Peripheral to the Big Timber Stock, Crazy Mountains, Montana

By Edward A. du Bray, Anna B. Wilson, and Bradley S. Van Gosen

Introduction

In the Crazy Mountains of south-central Montana, the Paleocene Fort Union Formation hosts a compositionally diverse array of Eocene plugs, dikes, and sills arrayed around the Eocene Big Timber stock; all of these rocks are part of the Crazy Mountains magmatic system. As documented by du Bray and Harlan (1996) and Dudas (1990, 1991), Eocene igneous rocks in the Crazy Mountains include silica-undersaturated, strongly alkaline intrusive rocks and silica-saturated, alkaline to subalkaline intrusive rocks that are approximately coeval. Most of the strongly alkaline rocks are in the northern part of the Crazy Mountains and form sills, laccoliths, small stocks, and dikes. The strongly alkaline plug at Ibex Mountain (fig. 1) is located significantly farther south than other strongly alkaline rocks associated with the Crazy Mountains magmatic system. Compositionally less exotic alkaline to subalkaline rocks, including constituents of the Big Timber stock (du Bray and Harlan, 1996), form stocks and associated dike swarms that are mostly restricted to the southern part of the range (fig. 1). Other Eocene intrusions, including outcrops at Gobblers Knob, Raspberry Butte, and other nearby conformable intrusions form a set of sills that are satellitic to the Big Timber stock and constitute a third, relatively unstudied set of intrusions in the Crazy Mountains (fig. 1).

The distribution of intrusive rocks in the Crazy Mountains is portrayed on various geologic maps of the area, including those by Wolff (1938), Simms (1966), Tappe (1966), Starmer (1972), and du Bray and others (1993). The petrology and petrogenesis of the strongly alkaline rocks in particular were well documented by Dudas (1990, 1991). Subsequently, du Bray and Harlan (1996) conducted a detailed investigation concerning the petrogenesis of the Big Timber stock, and du Bray and others (2006) characterized the radial dike swarm associated with the Big Timber stock. None of these studies, however, have documented and synthesized the geochemistry and petrography of the sills that are peripheral to the Big Timber stock.

The purpose of this report is (1) to present available geochemical and petrographic data for several dozen igneous rock samples, which represent sills and plugs peripheral to the Big Timber stock, and (2) to provide a basic interpretive synthesis of these data. These samples were collected in 1992 during geologic mapping of the Big Timber stock by du Bray and others (1993). During field studies, 28 outcrop samples were collected for subsequent laboratory analysis. Petrographic data were acquired for 25 of these samples, and geochemical analyses were acquired for 26 of these samples. Five samples of strongly alkaline rock, four from the plug at Ibex Mountain and one from a small plug exposed along the Shields River northwest of the Big Timber stock, are petrographically and geochemically distinct relative to all other samples described herein.

Analytical Methods

Petrographic characteristics of samples were determined using a standard petrographic microscope. All whole-rock major oxide chemical abundances were determined by wavelength-dispersive X-ray fluorescence spectrometry, using methods described by Taggart and others (1987), in analytical laboratories of the U.S. Geological Survey, Denver, Colorado. All iron abundances were converted to ferrous iron, and each major oxide analysis was recalculated to 100 percent on a volatile-free basis. Trace-element abundances were determined by energy-dispersive X-ray fluorescence spectroscopy (Elsass and du Bray, 1982; Yager and Quick, 1992) using ^{109}Cd and ^{241}Am radio-isotope excitation sources. All censored values were replaced by blank cells; for lower limits of determination, see Elsass and du Bray (1982).

Data Fields

Data were compiled using Microsoft Excel; they are presented here in two appendixes, found both at the back of this report and as Excel files (Appendix1.xlsx and Appendix2.xlsx) linked from this document and from *http://dx.doi.org/10.3133/ds895*. The files can be accessed using software

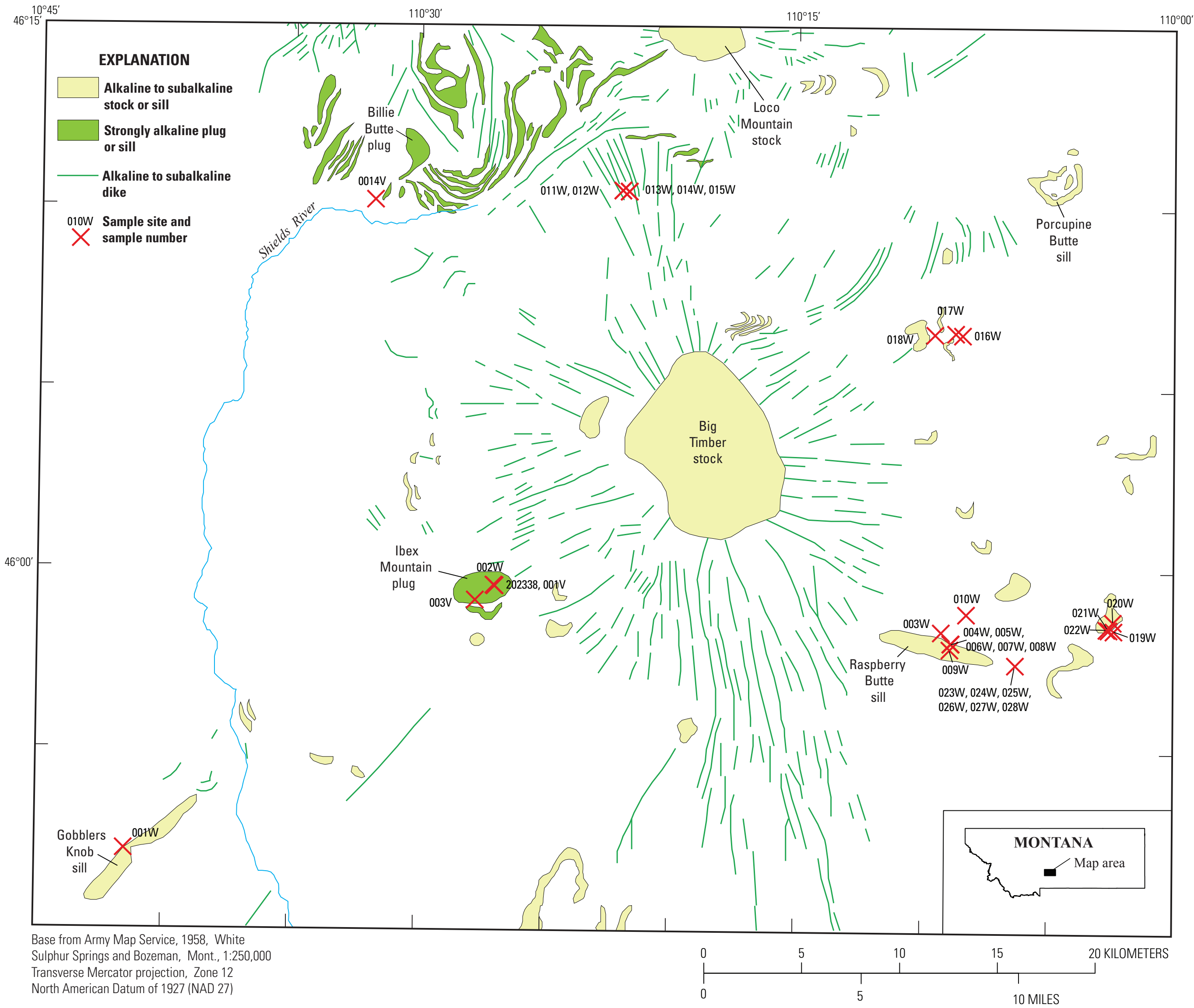

Figure 1. Regional geologic setting for the Crazy Mountains, Montana, showing the Big Timber stock, associated radial dikes, and peripheral sills and plugs. Collection sites for all samples described herein are labelled; complete sample numbers for samples ending in "V" or "W" include the suffix "92." Geologic features modified from Roberts (1972). (*Click here to open full-size, high-resolution image.*)

compatible with the .xlsx file format. Sample characterization, geochemical, and petrographic data are presented in columns or sets of related columns. The contents of appendix 1 constitute basic sample information, including sample location, sample treatment, and lithologic characterization for each sample; see table 1 for data field definitions. Appendix 2 contains geochemical and petrographic observations; see table 2 for data field definitions. Geochemical data in some worksheet cells might appear to be more precise than displayed values, but the implied precision is a misleading artifact of computational processes used to create data-cell contents (for instance, recalculation to 100-percent volatile free). Blank cells in the appendix worksheets indicate either null values or that no data are available. In appendix 2, some blank cells reflect abundances that were reported as "less than the lower limit of determination for the analytical method used;" these values were replaced by blank cells to enable statistical analysis of the uncensored data.

Geochemical Characteristics

Major Oxide Data

As is true of the Big Timber stock and its associated radial dike swarm (du Bray and Harlan, 1996; du Bray and others, 2006), major oxide characteristics of the sill-forming rocks peripheral to the Big Timber stock are consistent with a subduction-related petrogenesis. Compositions of three samples of the Ibex Mountain plug and one sample from a plug along the Shields River are quite distinct and are described separately. Relative to standard metrics (in cited sources), the sill-forming rocks are metaluminous (fig. 2) (Shand, 1951), magnesian (fig. 3) (Frost and others, 2001), and have compositions (fig. 4) that straddle the alkaline-subalkaline dividing line of Irvine and Baragar (1971). In terms of the balance between abundances of CaO, Na_2O, and K_2O in these rocks, the sill compositions vary significantly across the entire calcic, calc-alkalic, alkali-calcic, and alkalic spectrum (fig. 5), likely a misleading consequence of post-magmatic alteration and alkali mobility experienced by these rocks. Abundances of SiO_2 in the sill-forming rocks range nearly continuously from about 46 to 63 weight percent (fig. 4), and their compositions range from basalt to dacite and their alkaline analogs. Concentrations of TiO_2 and MgO vary considerably at lower SiO_2 abundances but scatter less and decrease to lower values at higher SiO_2 contents (fig. 6). Concentrations of FeO* (total iron, expressed in the ferrous state), MnO, and CaO (fig. 6) decrease in a linear fashion with increasing SiO_2. Abundances of Na_2O and P_2O_5 vary widely and yield no consistent variation relative to SiO_2 content. Abundances of Al_2O_3 and K_2O increase broadly with increasing SiO_2 content; the K_2O data array is dominated by transitional high-potassium to shoshonitic compositions (Gill, 1981). These trends and compositional ranges are similar to and overlap those of the Big Timber stock and its associated radial dike swarm (du Bray and Harlan, 1996; du Bray and others, 2006).

Primary mafic magmas that assimilate crustal contaminants predictably evolve to more silicic compositions characterized by progressively lower P_2O_5/K_2O because crustal materials generally have P_2O_5/K_2O less than 0.1 (Farmer and others, 2002). Among the sill-forming rocks, P_2O_5/K_2O decreases with increasing SiO_2 content and increases with increasing MgO content, which suggests that compositions of the magmas represented by these rocks evolved through variable contamination of primary mafic partial melts by crustally derived inputs. Similarly, Cousens and others (2008) suggested that decreasing CaO/Al_2O_3 with increasing SiO_2 principally reflects crustal contamination. Among the sill-forming rocks, CaO/Al_2O_3 decreases with increasing SiO_2, which corroborates the influence of progressive crustal contamination in the development of these rocks.

Table 1. Definition and characterization of data fields included in appendix 1 (status and treatment of samples).

FIELD_NAME	FIELD_DESCRIPTION
Field_ID	Field-assigned sample identifier; Field_ID entries may link data in individual rows to the contents of particular rows in the other appendix or to the National Geochemical Database.
Longitude	In decimal degrees, relative to the North American Datum of 1927. Longitude is reported as a negative value (western hemisphere).
Latitude	In decimal degrees, relative to the North American Datum of 1927. Latitude is reported as a positive value (northern hemisphere).
Chem	"X" indicates chemical analysis for sample obtained (see appendix 2).
TS	"X" indicates thin section of sample prepared and examined using a petrographic microscope (see appendix 2).
Locality_name	Prominent geographic feature proximal to sample site(s).
Lithology	Sample composition according to the classification scheme of Le Maitre (2002).
Igneous_form	Form (sill, dike, or plug) of the igneous rock represented by each sample.
Alteration	Geochemical characteristics indicative of alteration; high LOI (loss on ignition) equates to values >3 weight percent, and low K_2O equates to values <0.5 weight percent.

Table 2. Definition and characterization of data fields included in appendix 2 (geochemical and petrographic data).

FIELD_NAME	FIELD_DESCRIPTION
Field_ID	Field-assigned sample identifier; Field_ID entries may link data in individual rows to the contents of particular rows in the other appendix or to the National Geochemical Database.
Locality_name	Prominent geographic feature proximal to sample site(s).
SiO2_pct	Silicon, as silicon dioxide, in weight percent; based on major oxide data recalculated to 100 percent on a volatile-free basis.
TiO2_pct	Titanium, as titanium dioxide, in weight percent; based on major oxide data recalculated to 100 percent on a volatile-free basis.
Al2O3_pct	Aluminum, as aluminum trioxide, in weight percent; based on major oxide data recalculated to 100 percent on a volatile-free basis.
FeO*_pct	Total iron, as ferrous oxide, in weight percent; based on major oxide data recalculated to 100 percent on a volatile-free basis.
MnO_pct	Manganese, as manganese oxide, in weight percent; based on major oxide data recalculated to 100 percent on a volatile-free basis.
MgO_pct	Magnesium, as magnesium oxide, in weight percent; based on major oxide data recalculated to 100 percent on a volatile-free basis.
CaO_pct	Calcium, as calcium oxide, in weight percent; based on major oxide data recalculated to 100 percent on a volatile-free basis.
Na2O_pct	Sodium, as sodium oxide, in weight percent; based on major oxide data recalculated to 100 percent on a volatile-free basis.
K2O_pct	Potassium, as potassium oxide, in weight percent; based on major oxide data recalculated to 100 percent on a volatile-free basis.
P2O5_pct	Phosphorus, as phosphorus pentoxide, in weight percent; based on major oxide data recalculated to 100 percent on a volatile-free basis.
LOI_pct	Volatile content lost on ignition, in weight percent.
Total_I_pct	Initial, pre-recalculation sum of oxide abundances, in weight percent.
Ba_ppm	Barium, in parts per million.
Rb_ppm	Rubidium, in parts per million.
Sr_ppm	Strontium, in parts per million.
Y_ppm	Yttrium, in parts per million.
Zr_ppm	Zirconium, in parts per million.
Nb_ppm	Niobium, in parts per million.
Th_ppm	Thorium, in parts per million.
Ga_ppm	Gallium, in parts per million.
La_ppm	Lanthanum, in parts per million.
Ce_ppm	Cerium, in parts per million.
Nd_ppm	Neodymium, in parts per million.
Cu_ppm	Copper, in parts per million.
Pb_ppm	Lead, in parts per million.
Zn_ppm	Zinc, in parts per million.
Sn_ppm	Tin, in parts per million.
W_ppm	Tungsten, in parts per million.
As_ppm	Arsenic, in parts per million.
Sb_ppm	Antimony, in parts per million.
Abd_Pl_phenos	Modal abundance of plagioclase phenocrysts relative to the whole rock, in volume percent.
Abd_GrnAmph_phenos	Modal abundance of green amphibole (magnesio-hornblende) phenocrysts relative to the whole rock, in volume percent.

Table 2. Definition and characterization of data fields included in appendix 2 (geochemical and petrographic data).—Continued

FIELD_NAME	FIELD_DESCRIPTION
Abd_BrnAmph_phenos	Modal abundance of brown amphibole (magnesio-hastingsite) phenocrysts relative to the whole rock, in volume percent.
Abd_Bt_phenos	Modal abundance of biotite phenocrysts relative to the whole rock, in volume percent—TR, trace amounts (<0.5 volume percent).
Abd_Cpx_phenos	Modal abundance of clinopyroxene phenocrysts relative to the whole rock, in volume percent.
Abd_Ol_phenos	Modal abundance of olivine phenocrysts relative to the whole rock, in volume percent—TR, trace amounts (<0.5 volume percent).
Abd_Opq	Modal abundance of opaque iron-titanium oxide minerals relative to the whole rock, in volume percent.
TotXtls	Microscope-based estimate of total phenocryst content relative to the whole rock, in volume percent.
ClrIndx	Microscope-based estimate of color index (sum of the abundances of hornblende, biotite, pyroxene, olivine, and opaque iron-titanium oxide minerals), in volume percent.
AgsPl	Microscope-based estimate of average grain size of plagioclase phenocrysts, in millimeters.
AgsGrnAmph	Microscope-based estimate of average grain size of green amphibole (magnesio-hornblende) phenocrysts, in millimeters.
AgsBrnAmph	Microscope-based estimate of average grain size of brown amphibole (magnesio-hastingsite) phenocrysts, in millimeters.
AgsBt	Microscope-based estimate of average grain size of biotite phenocrysts, in millimeters.
AgsCpx	Microscope-based estimate of average grain size of clinopyroxene phenocrysts, in millimeters.
AgsOl	Microscope-based estimate of average grain size of olivine phenocrysts, in millimeters.
AgsOpq	Microscope-based estimate of average grain size of opaque iron-titanium oxide phenocrysts, in millimeters.
MgsPl	Microscope-based estimate of maximum grain size (length) of largest plagioclase phenocryst, in millimeters.
MgsGrnAmph	Microscope-based estimate of maximum grain size (length) of largest green amphibole (magnesio-hornblende) phenocryst, in millimeters.
MgsBrnAmph	Microscope-based estimate of maximum grain size (length) of largest brown amphibole (magnesio-hastingsite) phenocryst, in millimeters.
MgsBt	Microscope-based estimate of maximum grain size (length) of largest biotite phenocryst, in millimeters.
MgsCpx	Microscope-based estimate of maximum grain size (length) of largest clinopyroxene phenocryst, in millimeters.
MgsOl	Microscope-based estimate of maximum grain size (length) of largest olivine phenocryst, in millimeters.
MgsOpq	Microscope-based estimate of maximum grain size (length) of largest opaque iron-titanium oxide phenocryst, in millimeters.
Texture	Characteristic petrographic textures as determined by microscopic observation—Aph, aphanitic; Hy, hyalophitic; Hc, holocrystalline; I, intersertal; E, equigranular; P, porphyritic; S, seriate; T, trachytic.
Access_Mnrls	Accessory minerals identified by microscopic observation; listed in order of decreasing abundance—Ap, apatite; Ttn, titanite.
XlPl	Microscope-based estimate of crystallinity of plagioclase phenocrysts—A, anhedral; S, subhedral; E, euhedral.
XlGrnAmph	Microscope-based estimate of crystallinity of green amphibole (magnesio-hornblende) phenocrysts—A, anhedral; S, subhedral; E, euhedral.
XlBrnAmph	Microscope-based estimate of crystallinity of brown amphibole (magnesio-hastingsite) phenocrysts—A, anhedral; S, subhedral; E, euhedral.
XlBt	Microscope-based estimate of crystallinity of biotite phenocrysts—A, anhedral; S, subhedral; E, euhedral.
XlCpx	Microscope-based estimate of crystallinity of clinopyroxene phenocrysts—A, anhedral; S, subhedral; E, euhedral. If more than one crystallinity type is present, the dominant form is listed first.
XlOl	Microscope-based estimate of crystallinity of olivine phenocrysts—A, anhedral; S, subhedral; E, euhedral.
XlOpq	Microscope-based estimate of crystallinity of opaque iron-titanium oxide phenocrysts—A, anhedral; S, subhedral; E, euhedral.

Table 2. Definition and characterization of data fields included in appendix 2 (geochemical and petrographic data).—Continued

FIELD_NAME	FIELD_DESCRIPTION
Petrog_Com	Groundmass characteristics and otherwise noteworthy features. Groundmass minerals include plagioclase (Pl), hornblende (Hbl), clinopyroxene (Cpx), biotite (Bt), quartz (Qtz), and opaque iron-titanium minerals (Opq). The presence of secondary, alteration minerals, including chlorite (Chl), calcite (Cc), or epidote (Ep), is noted. [%, percent; mm, millimeters]
HblClr	Pleochroic colors of hornblende phenocrysts, if present.
AltExtnt	Microscope-based estimate of the extent of alteration—1 indicates a completely fresh sample, and 5 indicates a completely altered sample in which primary textures and minerals are not identifiable. Intermediate values of 2 through 4 identify progressively more altered samples.

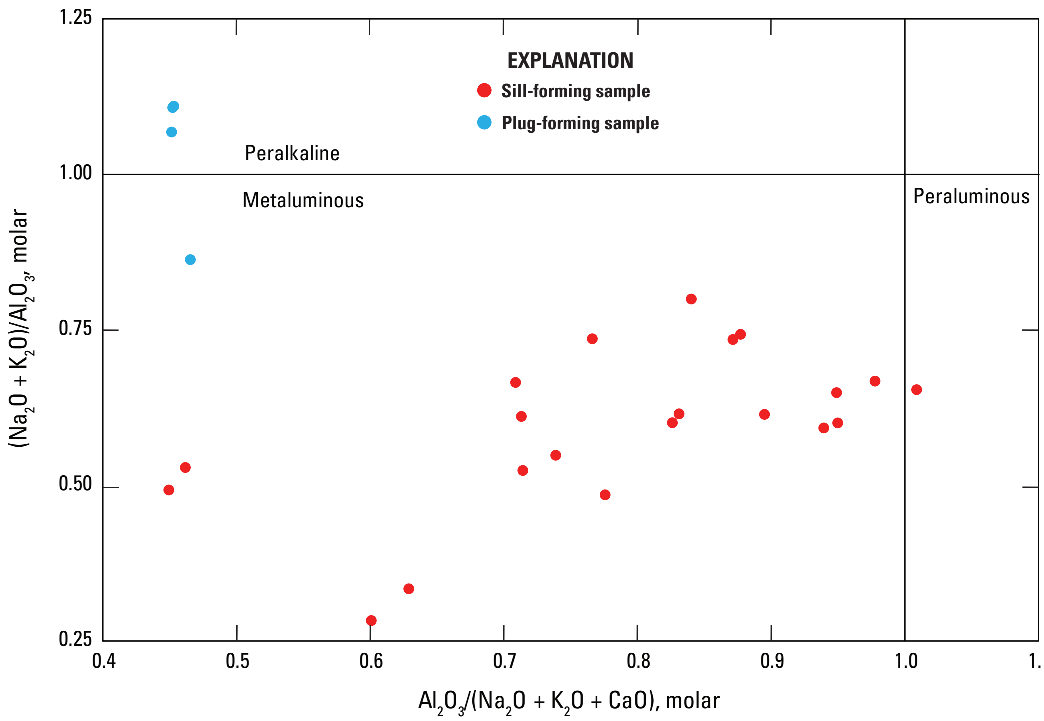

Figure 2. Variation diagram showing relative alumina and alkali saturation of igneous rocks peripheral to the Big Timber stock, Crazy Mountains, Montana, as a function of molar major-oxide compositions.

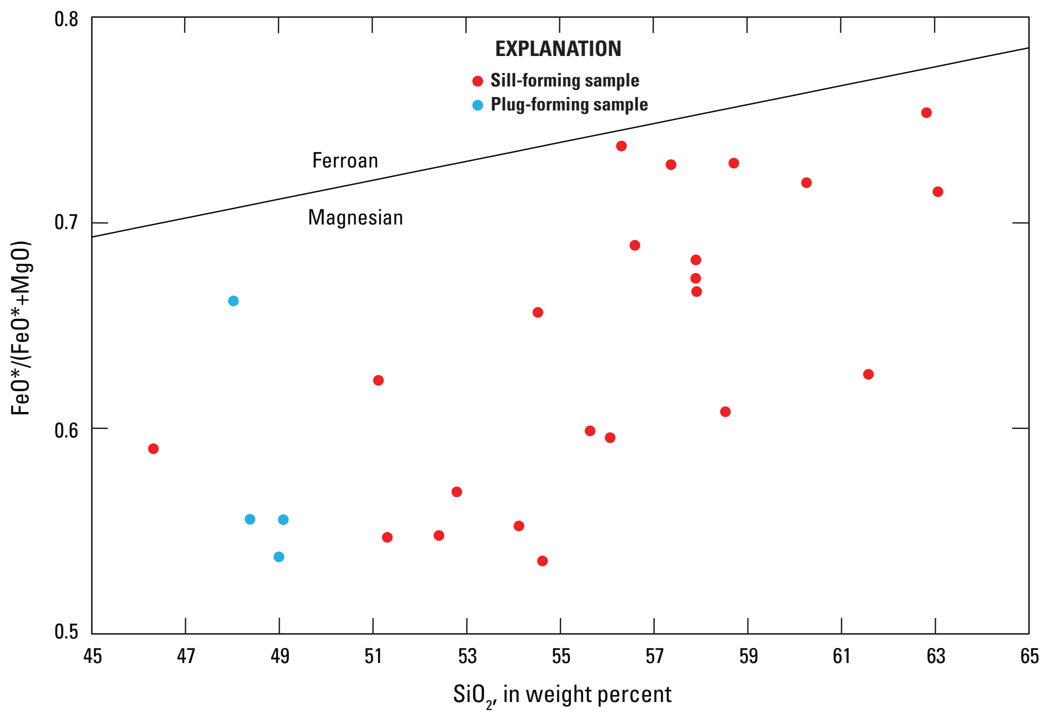

Figure 3. Variation diagram showing FeO/(FeO+MgO) values for igneous rocks peripheral to the Big Timber stock, Crazy Mountains, Montana, relative to boundaries between ferroan and magnesian rocks. Ferroan-magnesian boundary from Frost and others (2001).

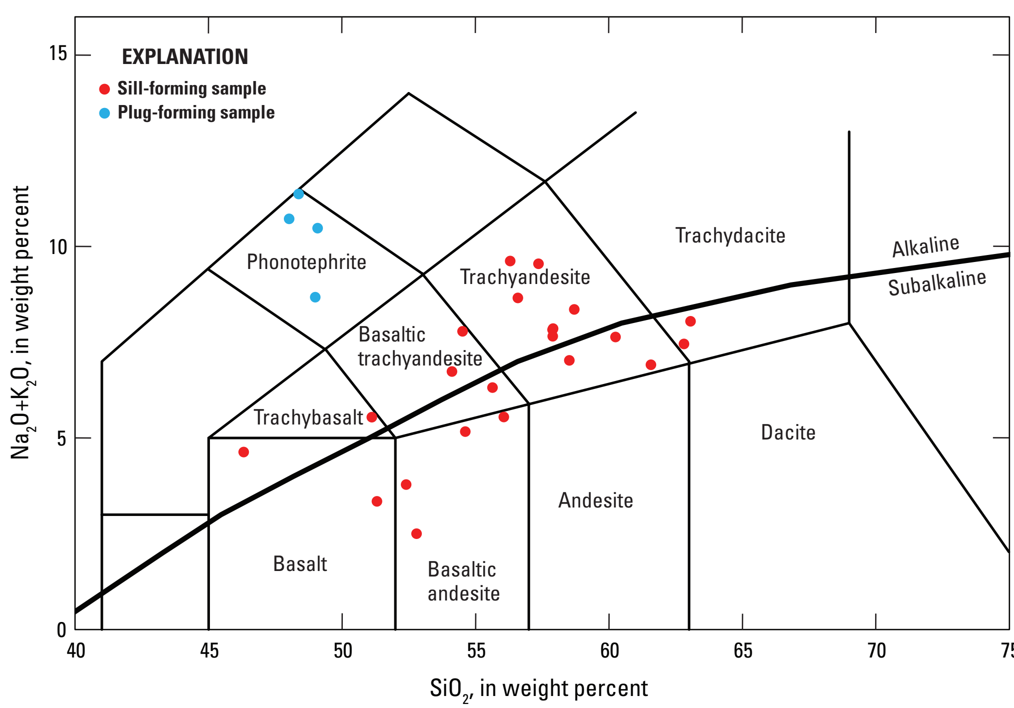

Figure 4. Total alkali-silica variation diagram showing compositions of igneous rocks peripheral to the Big Timber stock, Crazy Mountains, Montana. Field boundaries from Le Maitre (2002). Alkaline-subalkaline dividing line from Irvine and Baragar (1971).

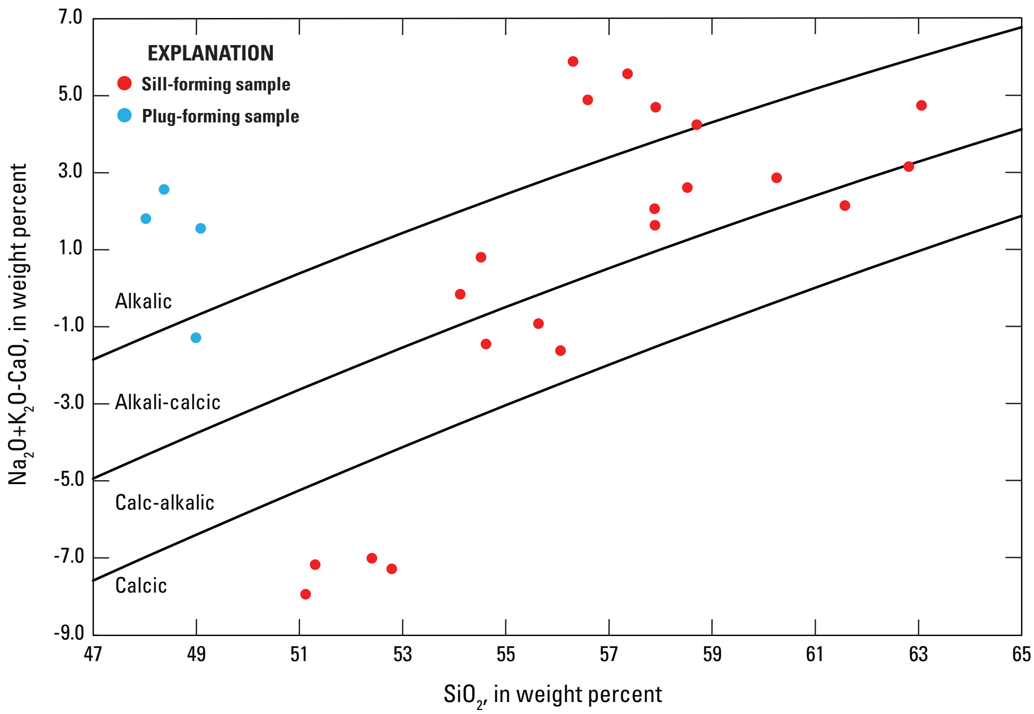

Figure 5. Variation diagram showing Na_2O+K_2O-CaO values versus SiO_2 content among samples of igneous rocks peripheral to the Big Timber stock, Crazy Mountains, Montana. Boundaries between various rock series from Frost and others (2001).

Many geochemical features distinguish the compositions of the samples of the Ibex Mountain and plugs along the Shields River (fig. 1) from those of the sill-forming rocks. First, all four of these representative samples are composed of phonotephrite and have strongly alkaline compositions (fig. 4) relative to the alkaline-subalkaline dividing line of Irvine and Baragar (1971). Three of these four samples have agpaitic indices greater than 1 (fig. 2) and are therefore peralkaline; the fourth contains aegirine, which is likewise diagnostic of peralkaline magmas. The silica content of these rocks, about 48 to 49 weight percent, is significantly lower than that of most of the sill-forming rocks. Both the Na_2O and K_2O contents of these rocks are elevated, given their low silica contents, but they are especially sodic, with Na_2O contents that range from about 5 to 8 weight percent (fig. 6). Like all other rocks in the Crazy Mountains, the strongly alkaline rocks are magnesian (fig. 3). Relative proportions of Na_2O, K_2O, and CaO in these rocks are consistent with alkalic to strongly alkali-calcic compositions (fig. 5). Relative to compositional trends depicted by all other alkaline to subalkaline rocks in the Crazy Mountains (fig. 6), the strongly alkaline rocks have low TiO_2 and CaO abundances, high Na_2O and K_2O abundances, and remarkably high P_2O_5 abundances (fig. 6). Their Al_2O_3, FeO, MnO, and MgO abundances are approximately on trend with those of other alkaline to subalkaline rocks in the Crazy Mountains.

Trace-Element Data

Several aspects of trace-element data available for sill-forming alkaline to subalkaline rocks of the Crazy Mountains are noteworthy. In particular, abundances of Ba (range, about 600–4,300 parts per million [ppm]; average, about 2,200) and Sr (range, about 400–1,400 ppm; average, about 900) in these rocks are especially elevated relative to the concentrations of those elements in most igneous rocks (Turekian and Wedepohl, 1961). Rubidium (Rb) abundances in these rocks are relatively low, resulting in very low Rb/Sr values (average, 0.06). Abundances of Y, Zr, Nb, La, Ce, and Nd in these rocks are similar to those of other convergent-margin, broadly calc-alkaline igneous rocks, such as those in the Andean, Kamchatka, and Central American volcanic arcs (Max Plank Institut für Chemie, 2010). Among the sill-forming rocks, Rb, Zr, La, and Ce abundances increase systematically with increasing silica content; Y abundances decrease; and Ba, Sr, Nb, and Nd abundances are uncorrelated with varying silica content. Most of the sill-forming rocks have relative abundances of Rb and Y+Nb that are consistent with a genesis in a volcanic arc setting (fig. 7).

Most continental magmatic arc rocks have Ba/Nb greater than 15 (Gill, 1981). The sill-forming rocks have Ba/Nb values that average about 126, range upward to almost 240, and do not vary systematically with respect to silica content.

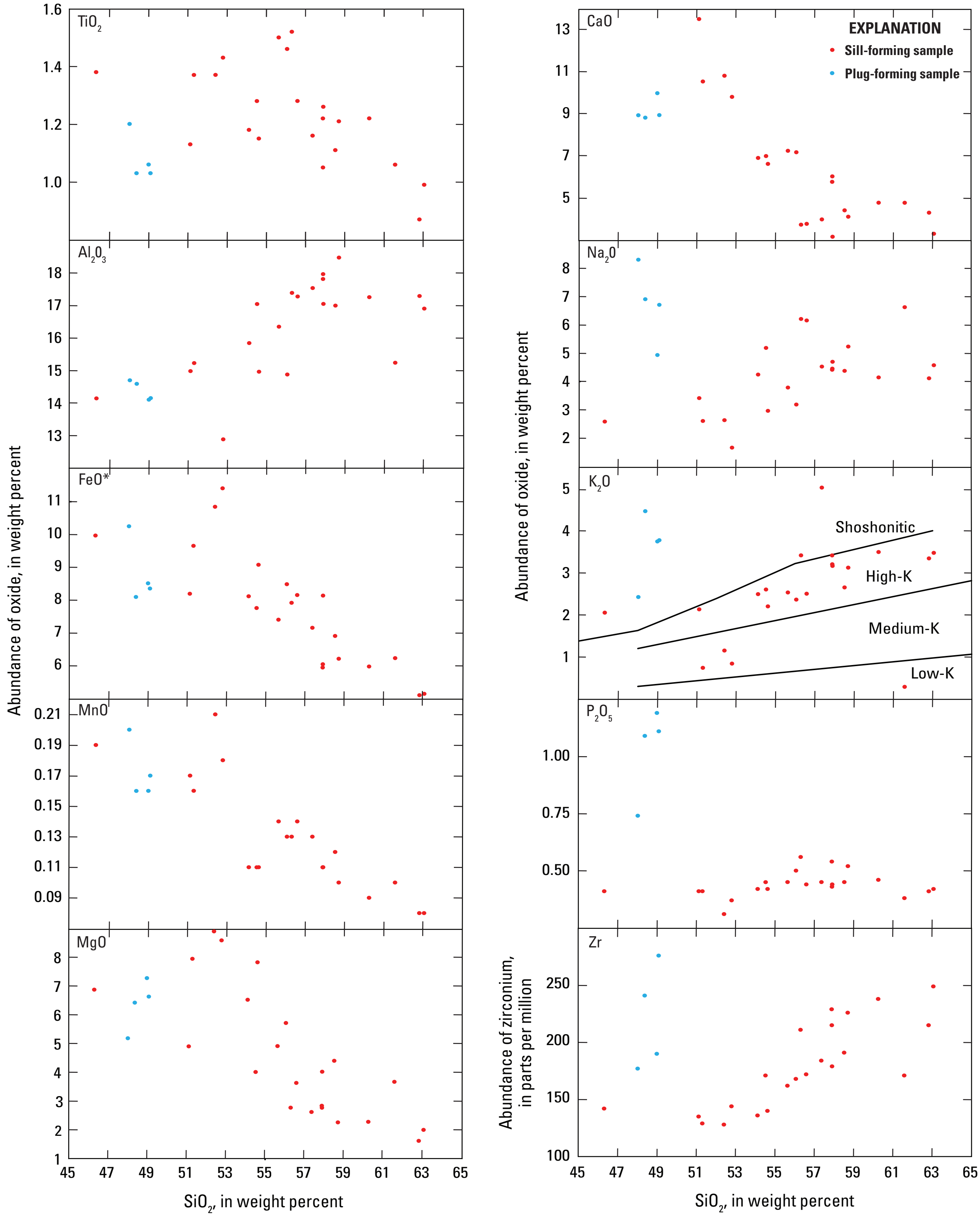

Figure 6. Variation diagrams showing abundances of major oxides in igneous rocks peripheral to the Big Timber stock, Crazy Mountains, Montana. All abundances in weight percent, except zirconium (in parts per million). Field boundaries on K_2O versus SiO_2 diagram from Le Maitre (2002); high-K–shoshonitic dividing line from Ewart (1982).

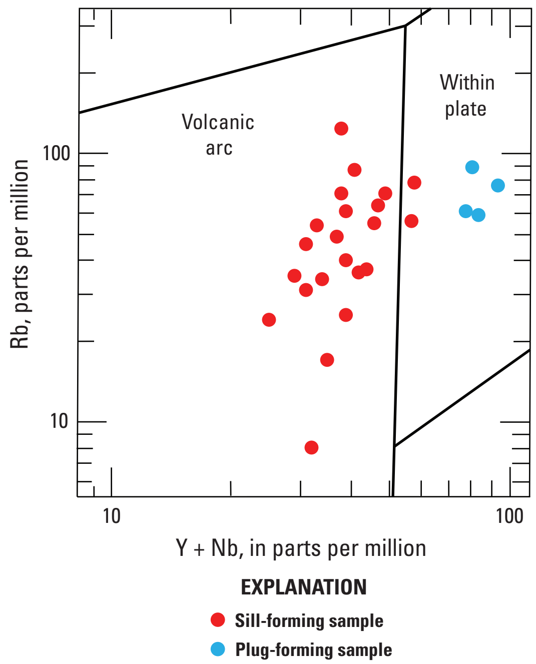

Figure 7. Trace-element, tectonic setting–discrimination variation diagram showing the composition of igneous rocks peripheral to the Big Timber stock, Crazy Mountains, Montana. Tectonic setting–composition boundaries from Pearce and others (1984).

Elevated Ba/Nb values have been associated with those mantle wedge magmas that derived subducted slab components through dehydration of the subducted-slab and attendant fluid flux–induced partial melting (Hawkesworth and others, 1995; Pearce and Peate, 1995; Cousens and others, 2008; Schmidt and others, 2008). Accordingly, highly elevated Ba/Nb ratios and noteworthy large-ion lithophile element (Ba and Sr) enrichments suggest significant involvement of a subducted-slab-derived fluid component in the petrogenesis of the magmas represented by the sill-forming rocks.

Trace-element characteristics of the strongly alkaline rocks are highly distinctive. Although Ba and Sr abundances in the sill-forming rocks are elevated (averaging about 3,200 and 2,700 ppm, respectively), those for the strongly alkaline rocks are even greater. Rubidium abundances in the strongly alkaline rocks are higher, averaging about 71 ppm; however, their average Rb/Sr ratio is even lower (0.03) than that for the sill-forming rocks. Similarly, Y, Zr, and Nb abundances of the strongly alkaline rocks are significantly higher than those of the sill-forming rocks. The average Zr content of the strongly alkaline rocks (221 ppm) is lower than might be expected given their alkalinity and experimental work by Watson (1979), which demonstrated that the alkaline magmas, such as those represented by these rocks, can contain significantly greater zirconium concentrations before zircon saturation is achieved and zirconium concentrations become buffered. Finally, the light rare earth element (La, Ce, and Nd) abundances of the strongly alkaline rocks are strikingly elevated relative to those characteristic of other igneous rocks (Turekian and Wedepohl, 1961). These trace-element characteristics suggest that the petrogenetic history of these alkaline rocks was quite different from that responsible for magmas represented by the sill-forming rocks. A significant aspect of these distinctive characteristics is underscored by the fact that relative abundances of Rb and Y+Nb for the strongly alkaline rocks coincide with the within-plate field on the trace-element, tectonic setting–discrimination variation diagram (fig. 7), whereas those for the sill-forming rocks are equivalent to volcanic arc compositions.

Petrographic Characteristics

Most samples of the sill-forming rocks described herein have similar petrographic characteristics; in contrast, samples of the strongly alkaline plug at Ibex Mountain are petrographically distinct and thus are described separately. Many of the sill-forming rocks contain either green or brown amphibole. Electron microprobe analyses of green and brown amphibole contained in the nearby Big Timber stock indicate that they are composed of magnesio-hornblende and magnesio-hastingsite, respectively (du Bray and Harlan, 1996). Optical features of the green amphibole in sill and Big Timber stock samples are indistinguishable, which suggests that the green amphibole in the sills is also magnesio-hornblende. Similarly, brown amphibole in the sills and the stock are optically indistinguishable, which suggests that brown amphibole in the sills is magnesio-hastingsite. The sill rocks are variably porphyritic. Phenocryst abundances range from 0 to 65 percent, averaging about 20 percent. Color index ranges from 1 to 35 percent, averaging about 13 percent. Fine- to medium-grained phenocryst assemblages include combinations of plagioclase, magnesio-hornblende, magnesio-hastingsite, clinopyroxene, and rare biotite in a fine-grained groundmass composed of combinations of plagioclase, magnesio-hornblende, magnesio-hastingsite, clinopyroxene, opaque iron-titanium oxides, and variably devitrified glass. The groundmass minerals form intersertal intergrowths in most samples, although in several samples the groundmass consists of intergranular intergrowths.

Among samples of dikes associated with the Big Timber stock, the composition of the mafic silicate minerals is strongly correlated with whole-rock composition (du Bray and others, 2006); basaltic trachyandesite dikes are dominated by clinopyroxene, low-silica trachyandesite dikes contain clinopyroxene and magnesio-hastingsite, high-silica trachyandesite to low-silica trachydacite dikes contain magnesio-hastingsite, and high-silica trachydacite to rhyolite dikes contain biotite and magnesio-hornblende. The composition of the mafic silicate minerals contained in the sill-forming rocks correlate similarly, but less systematically, with whole-rock composition. Accessory minerals in the sill-forming rocks are rare, though apatite was identified in several samples. The groundmass of many samples contains secondary calcite and (or) chlorite related to post magmatic alteration of many of these rocks. Similarly, many primary phenocrysts are variably altered and have been replaced by calcite and clay or sericite.

The plug at Ibex Mountain is composed of rock that ranges from holocrystalline and equigranular (sample 202338) to porphyritic with a hyalophitic groundmass (sample 002W92). Pale green clinopyroxene is the dominant mineral in both of these samples; other mafic silicate minerals include tan to distinctly red-brown biotite and trace amounts of subhedral olivine. Clinopyroxene in sample 202338 is overgrown by distinctive emerald-green aegirine rims, and in both Ibex Mountain samples is distinguished by a well-developed sieve texture. These rocks lack quartz and feldspar but, befitting their strongly alkaline character, they contain nepheline, which forms anhedral, interstitial grains in sample 202338 and euhedral phenocrysts in sample 002W92. Some nepheline is partly replaced by and (or) overgrown by acicular sprays of zeolite minerals. Sample 002W92 is further distinguished by the presence of cancrinite, which forms small discrete grains and overgrowths on nepheline crystals. The occurrence of cancrinite in strongly alkaline rocks, particularly in the northern Crazy Mountains, was highlighted by the detailed investigations of Simms (1966). Apatite is a characteristic accessory constituent of the Ibex Mountain plug.

Synthesis

The most significant finding derived from data presented herein is that the geochemical and petrographic characteristics of the sill-forming rocks are indistinguishable from those of the Big Timber stock and its radial dike swarm. Consequently, the central stock, associated radial dikes, and surrounding sills seem to be part of a single, coeval magmatic episode in the Crazy Mountains. By analogy, other still unsampled and undocumented sill-forming intrusions peripheral to and south and east of the Big Timber stock are probably also composed of rock related to magmatism responsible for formation of the Big Timber stock. In contrast, the small amount of data for the plug-forming rocks at Ibex Mountain and along the Shields River indicate that the geochemistry and petrography of these rocks are significantly different from those of the sill-forming rocks but remarkably similar to those of other strongly alkaline igneous rocks exposed north and west of the Big Timber stock.

Characteristics of the sill-forming intrusions are in accord with their petrogenesis in a subduction-related setting, as is also true for the Big Timber stock and its radial dike swarm (du Bray and Harlan, 1996). Unusual trace-element abundances, especially elevated concentrations of Ba and Sr, are consistent with significant crustal inputs through assimilation and (or) magmatism involving noteworthy inputs derived from fluids released during devolatilization of the downgoing, subducted slab. Finally, the geospatial and temporal coincidence of strongly alkaline and alkaline to subalkaline magmas in the Crazy Mountains remains something of a petrologic paradox.

Acknowledgments

Data compilation undertaken for this study was conducted as part of the mineral resource assessment of Custer and Gallatin National Forests funded by the U.S. Geological Survey Mineral Resources Program. Constructive reviews by Ryan D. Taylor and Matthew Granitto are much appreciated and helped clarify data presentation.

References Cited

Cousens, B.L., Prytulak, Julie, Henry, C.D., Alcazar, Al, and Brownrigg, Tim, 2008, Geology, geochronology, and geochemistry of the Miocene-Pliocene ancestral Cascades arc, northern Sierra Nevada, California and Nevada—The roles of the upper mantle, subducting slab, and the Sierra Nevada lithosphere: Geosphere, v. 4, p. 814–828.

du Bray, E.A., Elliott, J.E., Wilson, A.B., Van Gosen, B.S., and Rosenberg, L.A., 1993, Geologic map of the Big Timber stock and vicinity, southern Crazy Mountains, Sweet Grass and Park Counties, south-central Montana: U.S. Geological Survey Miscellaneous Field Investigations Series Map MF-2253, scale 1:24,000.

du Bray, E.A., and Harlan, S.S., 1996, The Eocene Big Timber stock, south-central Montana—Development of extensive compositional variation in an arc-related intrusion by side-wall crystallization and cumulate glomerocryst remixing: Geological Society of America Bulletin, v. 108, p. 1404–1424.

du Bray, E.A., Harlan, S.S., and Wilson, A.B., 2006, Petrology of the Crazy Mountains dike swarm and geochronology of associated sills, south-central Montana: U.S. Geological Survey Professional Paper 1715, 21 p.

Dudas, F.O., 1990, Petrogenesis and mantle source of igneous rocks in the Crazy Mountains, Montana: University Park, Pennsylvania State University, Ph.D. thesis, 442 p.

Dudas, F.O., 1991, Geochemistry of igneous rocks from the Crazy Mountains, Montana, and tectonic models for the Montana alkalic province: Journal of Geophysical Research, v. 96, p. 13261–13277.

Elsass, Françoise, and du Bray, E.A., 1982, Energy-dispersive X-ray fluorescence spectrometry with the Kevex 7000 system: Saudi Arabia, Deputy Ministry of Mineral Resources Open-File Report USGS-OF-02-52, 53 p.

Ewart, Anthony, 1982, The mineralogy and petrology of Tertiary—Recent orogenic volcanic rocks with special reference to the andesitic-basaltic compositional range, *in* Thorpe, R.S., ed., Andesites: New York, John Wiley and Sons, p. 25–87.

Farmer, G.L., Glazner, A.F., and Manley, C.R., 2002, Did lithospheric delamination trigger late Cenozoic potassic volcanism in the southern Sierra Nevada, California?: Geological Society of America Bulletin, v. 114, p. 754–768.

Frost, B.R., Barnes, C.G., Collins, W.J., Arculus, R.J., Ellis, D.J., and Frost, C.D., 2001, A geochemical classification for granitic rocks: Journal of Petrology, v. 42, p. 2033–2048.

Gill, J.B., 1981, Orogenic andesites and plate tectonics: New York, Springer-Verlag, 390 p.

Hawkesworth, Chris; Turner, Simon; Gallagher, Kerry; Hunter, Arlene; Bradshaw, Tim; and Rogers, Nick, 1995, Calc-alkaline magmatism, lithospheric thinning and extension in the Basin and Range: Journal of Geophysical Research, v. 100, p. 10271–10286.

Irvine, T.N., and Baragar, W.R.A., 1971, A guide to the chemical classification of the common volcanic rocks: Canadian Journal of Earth Sciences, v. 8, p. 523–548.

Le Maitre, R.W., 2002, Igneous rocks—A classification and glossary of terms (2d ed.): Cambridge, United Kingdom, Cambridge University Press, 236 p.

Max Plank Institut für Chemie, 2010, Geochemistry of rocks of the oceans and continents (GEOROC) [Query by geological setting—convergent margins]: Mainz, Germany, Max Plank Institut für Chemie, accessed June 10, 2014, at *http://georoc.mpch-mainz.gwdg.de/georoc/*.

Pearce, J.A., Harris, N.B.W., and Tindle, A.G., 1984, Trace element discrimination diagrams for the tectonic interpretation of granitic rocks: Journal of Petrology, v. 25, p. 956–983.

Pearce, J.A., and Peate, D.W., 1995, Tectonic implications of the composition of volcanic arc magmas: Annual Review of Earth and Planetary Sciences, v. 23, p. 251–285.

Roberts, A.E., 1972, Cretaceous and early Tertiary depositional and tectonic history of the Livingston area, southwestern Montana: U.S. Geological Survey Professional Paper 526-C, 120 p.

Schmidt, M.E., Grunder, A.L., and Rowe, M.C., 2008, Segmentation of the Cascade arc as indicated by Sr and Nd isotopic variation among diverse primitive basalts: Earth and Planetary Science Letters, v. 266, p. 166–181.

Shand, S.J., 1951, Eruptive rocks: New York, John Wiley, 488 p.

Simms, F.E., 1966, The igneous petrology, geochemistry, and structural geology of part of the northwestern Crazy Mountains, Montana: Cincinnati, Ohio, University of Cincinnati, Ph.D. thesis, 339 p.

Starmer, R.J., 1972, The distribution and geochemistry of the Big Timber dike swarm, Crazy Mountains, Montana: Cincinnati, Ohio, University of Cincinnati, Ph.D. thesis, 90 p.

Taggart, J.E., Lindsay, J.R., Scott, B.A., Vivit, D.V., Bartel, A.J., and Stewart, K.C., 1987, Analysis of geologic materials by X-ray fluorescence spectrometry, Chapter E *of* Baedecker, P.A., ed., Methods for geochemical analysis: U.S. Geological Survey Bulletin 1770, p. E1–E19.

Tappe, John, 1966, The chemistry, petrology, and structure of the Big Timber igneous complex, Crazy Mountains, Montana: Cincinnati, Ohio, University of Cincinnati, Ph.D. thesis, 134 p.

Turekian, K.K., and Wedepohl, K.H., 1961, Distribution of the elements in some major units of the Earth's crust: Geological Society of America Bulletin, v. 72, p. 175–192.

Watson, E.B., 1979, Zircon saturation in felsic liquids—Experimental results and applications to trace element geochemistry: Contributions to Mineralogy and Petrology, v. 70, p. 407–419.

Wolff, J.E., 1938, Igneous rocks of the Crazy Mountains, Montana: Geological Society of America Bulletin, v. 49, p. 1569–1626.

Yager, D.B., and Quick, J.E., 1992, SUPERXAP manual: U.S. Geological Survey Open-File Report 92-13, 45 p.

Publishing support provided by:
Denver Publishing Service Center

For more information concerning this publication, contact:
Center Director, USGS Central Mineral and Environmental Resources Science Center
Box 25046, Mail Stop 973
Denver, CO 80225
(303) 236-1562

Or visit the Central Mineral and Environmental Resources Science Center Web site at:
http://minerals.cr.usgs.gov/

Appendixes

Appendix 1. Status and treatment of samples of sills and plugs peripheral to the Big Timber stock, Crazy Mountains, Montana.
(Click here to open in Microsoft Excel.)

[See table 1 for an explanation of data fields. Chem, chemical analysis; TS, thin section; LOI, loss on ignition; K_2O, potassium oxide]

Field_ID	Longitude	Latitude	Chem	TS	Locality_name	Lithology	Ignous_form	Alteration
202338	–110.448	45.993	X	X	Ibex Mountain	Phonotephrite	Plug	
001V92	–110.448	45.993	X		Ibex Mountain	Phonotephrite	Plug	
003V92	–110.461	45.987	X		Ibex Mountain	Phonotephrite	Plug	
0014V92	–110.530	46.171	X		Shields River Road	Phonotephrite	Plug	high LOI
001W92	–110.691	45.871	X	X	Gobblers Knob	Trachyandesite	Sill	
002W92	–110.449	45.994		X	Ibex Mountain		Plug	
003W92	–110.153	45.973		X	Raspberry Butte		Sill	
005W92	–110.147	45.968	X	X	Raspberry Butte	Trachydacite	Sill	
006W92	–110.147	45.968	X	X	Raspberry Butte	Basaltic trachyandesite	Sill	
007W92	–110.147	45.968	X	X	Raspberry Butte	Trachydacite	Sill	
008W92	–110.147	45.968	X	X	Raspberry Butte	Trachyandesite	Sill	
009W92	–110.148	45.965	X	X	Raspberry Butte	Trachyandesite	Sill	
010W92	–110.137	45.981	X	X	Raspberry Butte	Trachyandesite	Sill	high LOI, low K_2O
011W92	–110.366	46.176	X	X	Loco Mountain	Basaltic trachyandesite	Dike	
012W92	–110.366	46.176	X	X	Loco Mountain	Trachyandesite	Dike	high LOI
014W92	–110.362	46.175	X	X	Loco Mountain	Trachyandesite	Dike	
015W92	–110.362	46.175	X	X	Loco Mountain	Basalt	Dike	high LOI
016W92	–110.140	46.110	X	X	Amelong Creek	Basaltic andesite	Sill	high LOI
017W92	–110.145	46.111	X	X	Amelong Creek	Trachyandesite	Sill	high LOI
018W92	–110.159	46.110	X	X	Amelong Creek	Trachyandesite	Sill	high LOI
019W92	–110.039	45.974	X	X	Grosfield Ranch	Basalt	Sill	high LOI
020W92	–110.040	45.978	X	X	Grosfield Ranch	Basaltic andesite	Sill	high LOI
021W92	–110.043	45.975	X	X	Grosfield Ranch	Basaltic trachyandesite	Sill	high LOI
022W92	–110.044	45.975	X	X	Grosfield Ranch	Trachybasalt	Sill	high LOI
024W92	–110.104	45.958	X	X	Grosfield Ranch	Trachyandesite	Sill	high LOI
025W92	–110.104	45.958	X	X	Grosfield Ranch	Basaltic andesite	Sill	high LOI
026W92	–110.104	45.958	X	X	Grosfield Ranch	Trachyandesite	Sill	high LOI
027W92	–110.104	45.958	X	X	Grosfield Ranch	Basaltic trachyandesite	Sill	high LOI

Appendix 2. Geochemical and petrographic data for samples of sills and plugs peripheral to the Big Timber stock, Crazy Mountains, Montana. *(Click here to open in Microsoft Excel.)*

[See table 2 for an explanation of data fields. mm, millimeter; pct, percent; ppm, parts per million; LOI, loss on ignition; Abd, abundance; phenos, phenocrysts; Ags, average grain size; Mgs, maximum grain size; Xl, crystallinity. Texture: Aph, aphanitic; E, equigranular; Hc, holocrystalline; Hy, hyalophitic; I, intersertal; P, porphyritic; S, seriate; T, trachytic. Accessory minerals: Ap, apatite, Ttn, titanite. Crystallinity: A, anhedral; E, euhedral; S, subhedral]

Field_ID	Locality_name	SiO2_pct	TiO2_pct	Al2O3_pct	FeO*_pct	MnO_pct	MgO_pct	CaO_pct	Na2O_pct	K2O_pct
202338	Ibex Mountain	49.00	1.06	14.10	8.51	0.16	7.33	9.97	4.93	3.74
001V92	Ibex Mountain	48.38	1.03	14.59	8.10	0.16	6.48	8.81	6.91	4.46
003V92	Ibex Mountain	49.09	1.03	14.15	8.35	0.17	6.69	8.93	6.71	3.77
014V92	Shields River Road	48.02	1.20	14.70	10.25	0.20	5.24	8.92	8.30	2.42
001W92	Gobblers Knob	57.89	1.22	17.81	5.95	0.11	2.89	5.76	4.41	3.41
002W92	Ibex Mountain									
003W92	Raspberry Butte									
005W92	Raspberry Butte	62.82	0.87	17.29	5.11	0.08	1.67	4.30	4.11	3.34
006W92	Raspberry Butte	55.64	1.50	16.35	7.41	0.14	4.97	7.24	3.78	2.53
007W92	Raspberry Butte	63.06	0.99	16.90	5.15	0.08	2.05	3.30	4.57	3.47
008W92	Raspberry Butte	57.89	1.05	17.96	6.05	0.11	2.82	6.02	4.45	3.20
009W92	Raspberry Butte	60.25	1.22	17.25	5.98	0.09	2.33	4.77	4.14	3.49
010W92	Raspberry Butte	61.58	1.06	15.24	6.23	0.10	3.72	4.77	6.62	0.29
011W92	Loco Mountain	52.79	1.43	12.89	11.41	0.18	8.64	9.79	1.66	0.84
012W92	Loco Mountain	57.36	1.16	17.54	7.16	0.13	2.67	3.98	4.52	5.02
014W92	Loco Mountain	56.31	1.52	17.39	7.92	0.13	2.82	3.73	6.21	3.41
015W92	Loco Mountain	51.31	1.37	15.23	9.65	0.16	8.00	10.52	2.60	0.74
016W92	Amelong Creek	56.06	1.46	14.88	8.49	0.13	5.77	7.17	3.18	2.36
017W92	Amelong Creek	58.52	1.11	16.99	6.91	0.12	4.45	4.41	4.37	2.65
018W92	Amelong Creek	58.70	1.21	18.47	6.21	0.10	2.31	4.11	5.23	3.12
019W92	Grosfield Ranch	46.32	1.38	14.14	9.97	0.19	6.93	16.03	2.58	2.05
020W92	Grosfield Ranch	54.62	1.15	14.96	9.08	0.11	7.88	6.62	2.96	2.20
021W92	Grosfield Ranch	54.12	1.18	15.84	8.12	0.11	6.58	6.90	4.24	2.49
022W92	Grosfield Ranch	51.12	1.13	14.98	8.20	0.17	4.95	13.49	3.41	2.13
024W92	Grosfield Ranch	57.91	1.26	17.05	8.14	0.11	4.07	3.16	4.69	3.16
025W92	Grosfield Ranch	52.41	1.37	11.32	10.84	0.21	8.95	10.79	2.63	1.15
026W92	Grosfield Ranch	56.59	1.28	17.28	8.16	0.14	3.68	3.77	6.16	2.50
027W92	Grosfield Ranch	54.52	1.28	17.04	7.76	0.11	4.06	6.99	5.18	2.60

Field_ID	Locality_name	P2O5_pct	LOI_pct	Total_I_pct	Ba_ppm	Rb_ppm	Sr_ppm	Y_ppm	Zr_ppm	Nb_ppm
202338	Ibex Mountain	1.19	2.76	97.94	3,000	61	3,152	38	190	40
001V92	Ibex Mountain	1.09	1.91	98.04	3,164	89	2,289	34	241	47
003V92	Ibex Mountain	1.11	2.51	98.10	3,215	76	2,415	38	276	56
014V92	Shields River Road	0.74	3.29	98.29	3,371	59	2,916	37	177	47
001W92	Gobblers Knob	0.54	1.39	98.60	2,225	78	1,272	24	229	34
002W92	Ibex Mountain									
003W92	Raspberry Butte									
005W92	Raspberry Butte	0.41	0.34	98.64	2,014	87	878	19	215	22
006W92	Raspberry Butte	0.45	0.61	98.67	1,634	55	827	23	162	23
007W92	Raspberry Butte	0.42	1.26	98.25	2,405	71	937	19	249	30
008W92	Raspberry Butte	0.43	0.32	98.40	2,287	64	1,204	24	215	23
009W92	Raspberry Butte	0.46	1.59	99.01	1,701	71	936	14	238	24
010W92	Raspberry Butte	0.38	5.29	99.14	627	8	1,170	9	171	23
011W92	Loco Mountain	0.37	2.64	99.32	1,001	24	600	15	144	10
012W92	Loco Mountain	0.45	3.39	98.81	2,272	124	1,019	20	184	18
014W92	Loco Mountain	0.56	1.32	98.80	2,969	56	1,592	26	211	31
015W92	Loco Mountain	0.41	5.75	99.33	799	17	739	22	129	13
016W92	Amelong Creek	0.50	4.81	99.17	1,254	37	740	25	168	19
017W92	Amelong Creek	0.45	5.22	98.90	2,011	46	568	16	191	15
018W92	Amelong Creek	0.52	3.71	98.56	2,734	61	1,033	19	226	20
019W92	Grosfield Ranch	0.41	12.70	98.49	1,929	31	720	18	142	13
020W92	Grosfield Ranch	0.42	8.34	98.77	2,662	35	431	18	140	11
021W92	Grosfield Ranch	0.42	8.13	98.55	4,254	40	716	21	136	18
022W92	Grosfield Ranch	0.41	10.40	98.63	3,176	34	907	19	135	15
024W92	Grosfield Ranch	0.44	4.30	98.41	4,331	54	703	17	179	16
025W92	Grosfield Ranch	0.31	3.11	99.67	1,574	25	480	27	128	12
026W92	Grosfield Ranch	0.44	3.50	98.72	2,446	36	1,382	26	172	16
027W92	Grosfield Ranch	0.45	6.27	98.57	2,921	49	807	18	171	19

Appendix 2. Geochemical and petrographic data for samples of sills and plugs peripheral to the Big Timber stock, Crazy Mountains, Montana.—Continued

[See table 2 for an explanation of data fields. mm, millimeter; pct, percent; ppm, parts per million; LOI, loss on ignition; Abd, abundance; phenos, phenocrysts; Ags, average grain size; Mgs, maximum grain size; Xl, crystallinity. Texture: Aph, aphanitic; E, equigranular; Hc, holocrystalline; Hy, hyalophitic; I, intersertal; P, porphyritic; S, seriate; T, trachytic. Accessory minerals: Ap, apatite, Ttn, titanite. Crystallinity: A, anhedral; E, euhedral; S, subhedral]

Field_ID	Locality_name	Th_ppm	Ga_ppm	La_ppm	Ce_ppm	Nd_ppm	Cu_ppm	Pb_ppm	Zn_ppm	Sn_ppm
202338	Ibex Mountain		12	164	236	137	122		74	5
001V92	Ibex Mountain		25	161	251	112	184	25	67	
003V92	Ibex Mountain		24	152	273	118	23	56	137	5
014V92	Shields River Road		17	151	283	170	197	22	156	2
001W92	Gobblers Knob		32	88	155	42	11	18	88	2
002W92	Ibex Mountain									
003W92	Raspberry Butte									
005W92	Raspberry Butte		14	57	108	54			71	7
006W92	Raspberry Butte			41	93	36		22	78	
007W92	Raspberry Butte		21	76	111	65	28	10	42	
008W92	Raspberry Butte		14	62	113	33		47	77	5
009W92	Raspberry Butte		20	48	94	49	9	24	69	7
010W92	Raspberry Butte		19	57	96	40	29	28	74	
011W92	Loco Mountain		9	20	60	40	28	32	99	
012W92	Loco Mountain		30	47	70	27	24	10	54	
014W92	Loco Mountain		26	43	83	62	2		104	2
015W92	Loco Mountain		26	32	67	26	55	30	79	
016W92	Amelong Creek			38	76	33	25	14	47	5
017W92	Amelong Creek		9	51	76	46	25	35	62	2
018W92	Amelong Creek		9	73	69	44	65	10	60	
019W92	Grosfield Ranch		25	48	78	51	49	29	93	
020W92	Grosfield Ranch		16	48	79	49	6	4	58	
021W92	Grosfield Ranch		19	36	74	29	22	42	60	
022W92	Grosfield Ranch		19	63	72	50	16	17	78	
024W92	Grosfield Ranch	10		44	50	22	8	26	80	
025W92	Grosfield Ranch	15	18	25	50	52	27	33	111	
026W92	Grosfield Ranch			33	80	36	63	20	46	
027W92	Grosfield Ranch	17	13	46	68	54	11	25	85	

Field_ID	Locality_name	W_ppm	As_ppm	Sb_ppm	Abd_Pl_phenos	Abd_GrnAmph_phenos	Abd_BrnAmph_phenos
202338	Ibex Mountain		16	0.4			
001V92	Ibex Mountain		6	0.3			
003V92	Ibex Mountain			0.2			
014V92	Shields River Road		14	0.4			
001W92	Gobblers Knob		8	0.2	20	5	
002W92	Ibex Mountain						
003W92	Raspberry Butte				15		10
005W92	Raspberry Butte		12	0.9	25		1
006W92	Raspberry Butte		2	0.4	3	8	5
007W92	Raspberry Butte			0.7	15	4	5
008W92	Raspberry Butte			0.4	15	3	2
009W92	Raspberry Butte	2		0.6	15	2	5
010W92	Raspberry Butte		28	0.6	4		
011W92	Loco Mountain			0.4			
012W92	Loco Mountain			0.4	7		2
014W92	Loco Mountain		16	1.2	40		25
015W92	Loco Mountain	2	0	0.6	7		
016W92	Amelong Creek		13	0.3	10		
017W92	Amelong Creek			0.3	25		
018W92	Amelong Creek			0.4	25		
019W92	Grosfield Ranch		20		1		
020W92	Grosfield Ranch		27				
021W92	Grosfield Ranch	4	10	0.3			
022W92	Grosfield Ranch		8	0.1			
024W92	Grosfield Ranch		15	0.3	3		
025W92	Grosfield Ranch		3	0.6	1		
026W92	Grosfield Ranch	1		0.2	5		
027W92	Grosfield Ranch		19	0.5	1		

Appendix 2. Geochemical and petrographic data for samples of sills and plugs peripheral to the Big Timber stock, Crazy Mountains, Montana.—Continued

Field_ID	Locality_name	Abd_Bt_phenos	Abd_Cpx_phenos	Abd_Ol_phenos	Abd_Opq	TotXtls	ClrIndx	AgsPl	AgsGrnAmph
202338	Ibex Mountain	10	40	TR	3	53	53		
001V92	Ibex Mountain								
003V92	Ibex Mountain								
014V92	Shields River Road								
001W92	Gobblers Knob	5	15		3	48	28	3.0	0.3
002W92	Ibex Mountain	3	30		2	44	35		
003W92	Raspberry Butte	TR			2	27	12	0.8	
005W92	Raspberry Butte				1	27	2	0.7	
006W92	Raspberry Butte				2	18	15	0.8	0.8
007W92	Raspberry Butte				3	27	12	1.2	0.5
008W92	Raspberry Butte				1	21	6	1.5	0.7
009W92	Raspberry Butte	TR			3	25	10	1.5	0.4
010W92	Raspberry Butte		6		1	11	7	1.5	
011W92	Loco Mountain		20		4	24	24		
012W92	Loco Mountain				3	12	5	1.0	
014W92	Loco Mountain				5	70	30	0.5	
015W92	Loco Mountain		5		3	15	8	1.0	
016W92	Amelong Creek		5		3	18	8	1.0	
017W92	Amelong Creek				2	27	2	1.0	
018W92	Amelong Creek				2	27	2	2.0	
019W92	Grosfield Ranch		15			16	15	0.8	
020W92	Grosfield Ranch		15		3	18	18		
021W92	Grosfield Ranch				2	2	2		
022W92	Grosfield Ranch		15		2	17	17		
024W92	Grosfield Ranch				3	6	3	1.5	
025W92	Grosfield Ranch		30		4	35	34	1.0	
026W92	Grosfield Ranch		1		4	10	5	2.0	
027W92	Grosfield Ranch				1	2	1	1.5	

Field_ID	Locality_name	AgsBrnAmph	AgsBt	AgsCpx	AgsOl	AgsOpq	MgsPl	MgsGrnAmph	MgsBrnAmph	MgsBt	MgsCpx
202338	Ibex Mountain		0.9	2.0	1.0	0.20				2.0	3.5
001V92	Ibex Mountain										
003V92	Ibex Mountain										
014V92	Shields River Road										
001W92	Gobblers Knob		0.5	0.7		0.20	4.0	1.2		1.5	3.5
002W92	Ibex Mountain		0.5	2.0		0.10				1.0	3.5
003W92	Raspberry Butte	0.8	0.4			0.05	2.5		2.0	0.4	
005W92	Raspberry Butte	1.0				0.10	2.5		2.0		
006W92	Raspberry Butte	0.6				0.04	2.0	2.0	1.5		
007W92	Raspberry Butte	0.5				0.10	2.5	1.5	2.0		
008W92	Raspberry Butte	0.5				0.10	3.5	2.8	1.5		
009W92	Raspberry Butte	0.5	0.4			0.10	2.8	0.5	2.0	0.4	
010W92	Raspberry Butte			0.5		0.03	1.5				1.0
011W92	Loco Mountain			2.0		0.05					4.5
012W92	Loco Mountain	0.4				0.10	4.0		0.5		
014W92	Loco Mountain	0.3				0.05	1.5		1.5		
015W92	Loco Mountain			1.0		0.02	2.8				3.5
016W92	Amelong Creek			1.5		0.03	4.5				2.5
017W92	Amelong Creek					0.05	2.0				
018W92	Amelong Creek					0.03	4.0				
019W92	Grosfield Ranch			2.0		0.01	1.4				4.0
020W92	Grosfield Ranch			0.5		0.02					1.5
021W92	Grosfield Ranch					0.03					
022W92	Grosfield Ranch			0.5		0.01					1.0
024W92	Grosfield Ranch					0.04	4.0				
025W92	Grosfield Ranch			2.5		0.10	2.0				7.0
026W92	Grosfield Ranch			0.8		0.04	3.2				1.5
027W92	Grosfield Ranch					0.15	2.5				

Appendix 2. Geochemical and petrographic data for samples of sills and plugs peripheral to the Big Timber stock, Crazy Mountains, Montana.—Continued

[See table 2 for an explanation of data fields. mm, millimeter; pct, percent; ppm, parts per million; LOI, loss on ignition; Abd, abundance; phenos, phenocrysts; Ags, average grain size; Mgs, maximum grain size; Xl, crystallinity. Texture: Aph, aphanitic; E, equigranular; Hc, holocrystalline; Hy, hyalophitic; I, intersertal; P, porphyritic; S, seriate; T, trachytic. Accessory minerals: Ap, apatite, Ttn, titanite. Crystallinity: A, anhedral; E, euhedral; S, subhedral]

Field_ID	Locality_name	MgsOl	MgsOpq	Texture	Access_Mnrls	XlPl	XlGrnAmph	XlBrnAmph	XlBt	XlCpx	XlOl	XlOpq
202338	Ibex Mountain	1.0	0.40	Hc; E	Ap				S	E	S	S
001V92	Ibex Mountain											
003V92	Ibex Mountain											
014V92	Shields River Road											
001W92	Gobblers Knob		0.40	Hc; P	Ap; Ttn	S	A		A	A; S		S
002W92	Ibex Mountain		0.50	Hy; P	Ap				E	E; S		A
003W92	Raspberry Butte		0.40	Hy; P; T		E		E	S			S
005W92	Raspberry Butte		0.40	Hy; P	Ap	S		S				A
006W92	Raspberry Butte		0.20	P		E	S	E				A
007W92	Raspberry Butte		0.40	P	Ap, Ttn	E	S	S				S
008W92	Raspberry Butte		0.20	P; I	Ap; Ttn	E	S	E				A
009W92	Raspberry Butte		0.20	P; Hy	Ap	E	S	S	S			S
010W92	Raspberry Butte		0.10	P; I	Ttn (secondary)	S				S		A
011W92	Loco Mountain		0.30	P; Hy	Ap					S		A
012W92	Loco Mountain		0.30	P; I	Ap	E		S				A
014W92	Loco Mountain		0.40	Aph; S		S		S				S
015W92	Loco Mountain		0.10	P; I		E				E		S
016W92	Amelong Creek		0.50	P; I		E				E		E
017W92	Amelong Creek		0.40	P; Hc	Ap	S						S
018W92	Amelong Creek		0.60	P; Hc	Ap	E						S
019W92	Grosfield Ranch		0.60	P; I		S				S		E
020W92	Grosfield Ranch		0.05	P; I						S		S
021W92	Grosfield Ranch		0.20	Aph; I								S
022W92	Grosfield Ranch		0.10	Aph; P						E		A
024W92	Grosfield Ranch		0.60	P; I		A						S
025W92	Grosfield Ranch		0.60	P; I		S				E		A
026W92	Grosfield Ranch		0.40	P; I		S				S		S
027W92	Grosfield Ranch		0.50	P; I	Ap?	S						A

Field_ID	Locality_name	Petrog_Com	HblClr	AltExtnt
202338	Ibex Mountain	Includes about 47% anhedral, interstitial nepheline (0.5–4.5 mm, average 1.5 mm); variably altered to zeolite minerals. Cpx includes distinctive emerald-green aegirine overgrowths.		1+
001V92	Ibex Mountain			
003V92	Ibex Mountain			
014V92	Shields River Road			
001W92	Gobblers Knob	Groundmass: clay-altered Pl (0.5 mm), Bt (0.4 mm), Qtz (0.3 mm), Hbl (0.3 mm), Cpx (0.3 mm), Opq (0.2 mm). Fine to medium grained. Hbl completely altered to Chl.		2+
002W92	Ibex Mountain	Groundmass: turbid, moderately devitrified glass. Rock also contains 7% 0.2–1.2 (0.5) mm nepheline and 2% 0.5–1.2 (0.9) mm cancrinite (0.5–1.2 mm, average 0.9 mm). Cpx strongly seive textured.		2
003W92	Raspberry Butte	Groundmass: moderately devitrified glass with Pl (0.1 mm), Hbl (0.05 mm), Opq (0.02 mm).	Pale tan to tan	1
005W92	Raspberry Butte	Groundmass: devitrified intergrowth of Pl (0.1 mm), Hbl (0.01 mm). Some secondary Chl.	Pale tan to tan	2
006W92	Raspberry Butte	Groundmass: intergranular intergrowth of Pl (0.1 mm), Cpx (0.01 mm), Opq (0.02 mm). Green amphibole completely altered to Chl.	Pale tan to tan	3
007W92	Raspberry Butte	Groundmass: intergranular intergrowth of Pl (0.2 mm), Opq (0.1 mm). Brown amphibole considerably altered to Chl. Green amphibole altered to Chl+Ep.	Pale tan to tan	3
008W92	Raspberry Butte	Groundmass: intersertal intergrowth of Pl (0.1 mm), Hbl (0.1 mm). Brown amphibole considerably altered to Chl. Green amphibole altered to Chl+Ep.	Brown amphibole: Pale tan to tan Green amphibole: Yellow green to green	2
009W92	Raspberry Butte	Groundmass: moderately devitrified glass with Pl (0.1 mm), Hbl (0.05 mm), Opq (0.02 mm). Green amphibole altered to Chl.	Brown amphibole: Pale tan to tan Green amphibole: Pale green	2-
010W92	Raspberry Butte	Groundmass: intersertal intergrowth of Pl (0.1 mm), altered/devitrified glass, Opq (0.03 mm). Pl almost completely replaced by Cc. Cpx, completely replaced by Cc + clay.		3+
011W92	Loco Mountain	Groundmass: intersertal intergrowth of altered (clay+Cc) Pl (0.2 mm), brown amphibole (0.05 mm), Chl, moderately devitrifed glass, Opq (0.05 mm). Cpx, moderately seived.		3

Appendix 2. Geochemical and petrographic data for samples of sills and plugs peripheral to the Big Timber stock, Crazy Mountains, Montana.—Continued

[See table 2 for an explanation of data fields. mm, millimeter; pct, percent; ppm, parts per million; LOI, loss on ignition; Abd, abundance; phenos, phenocrysts; Ags, average grain size; Mgs, maximum grain size; Xl, crystallinity. Texture: Aph, aphanitic; E, equigranular; Hc, holocrystalline; Hy, hyalophitic; I, intersertal; P, porphyritic; S, seriate; T, trachytic. Accessory minerals: Ap, apatite, Ttn, titanite. Crystallinity: A, anhedral; E, euhedral; S, subhedral]

Field_ID	Locality_name	Petrog_Com	HblClr	AltExtnt
012W92	Loco Mountain	Groundmass: intersertal intergrowth of Pl (0.1 mm), brown amphibole (0.1 mm), Opq (0.04 mm). Abundant secondary Cc.	Pale tan to tan	3+
014W92	Loco Mountain	Groundmass: intersertal intergrowth of Pl (0.1 mm), brown amphibole (0.1 mm), moderately devitrified glass, Opq (0.03 mm).	Pale tan to tan	2
015W92	Loco Mountain	Groundmass: intersertal intergrowth of Pl (0.1 mm), brown amphibole (0.05 mm), Opq (0.03 mm). Abundant secondary Cc; some secondary Chl.		3
016W92	Amelong Creek	Groundmass: intersertal intergrowth of Pl (0.1 mm), brown amphibole (0.1 mm), Opq (0.03 mm). Abundant secondary Cc; some secondary Chl.		2+
017W92	Amelong Creek	Groundmass: intersertal intergrowth of Pl (0.2 mm), brown amphibole (0.1 mm), Opq (0.05 mm). Abundant secondary Cc and Chl.		3
018W92	Amelong Creek	Groundmass: intersertal intergrowth of Pl (0.2 mm), Hbl (0.1 mm), Qtz (0.05 mm), Opq (0.02 mm). Abundant secondary Chl.		3
019W92	Grosfield Ranch	Groundmass: intersertal intergrowth of Pl (0.1 mm), brown amphibole (0.05 mm), Opq (0.01 mm). Abundant secondary Chl and Qtz.		3
020W92	Grosfield Ranch	Groundmass: intersertal intergrowth of Pl (0.1 mm), Hbl (0.05 mm), turbid glass, Opq (0.02 mm). Cpx completely altered to Chl+clay. Abundant secondary Chl and Qtz.		3+
021W92	Grosfield Ranch	Groundmass: intersertal intergrowth of Pl (0.2 mm), Hbl (0.1 mm), Opq (0.03 mm). Rock may have contained phenocrysts; if so, phenocrysts obliterated by alteration.		3+
022W92	Grosfield Ranch	Groundmass: aphanitic intergrowth of Pl (0.05 mm), Opq (0.01 mm), altered/devitrified glass.		4
024W92	Grosfield Ranch	Groundmass: intersertal intergrowth of Pl (0.4 mm), Hbl (0.1 mm), Opq (0.05 mm). Abundant secondary Cc.		2+
025W92	Grosfield Ranch	Groundmass: intersertal intergrowth of Pl (0.2 mm), Hbl (0.2 mm), Opq (0.05 mm), Cpx (0.1 mm).		2-
026W92	Grosfield Ranch	Groundmass: intersertal intergrowth of Pl (0.3 mm), Hbl (0.1 mm), Cpx (0.1 mm), Opq (0.04 mm).		3
027W92	Grosfield Ranch	Groundmass: intersertal intergrowth of Pl (0.2 mm), Hbl (0.1 mm), Opq (0.04 mm), devitrified glass (?). Abundant secondary Cc. Hbl in ground-mass altered to Chl.		3

USGS

du Bray and others—**Geochemical and Petrographic Data for Intrusions Peripheral to the Big Timber Stock, Crazy Mountains, Montana**—Data Series 895

ISSN 2327-638X (online)
http://dx.doi.org/10.3133/ds895